ChemComm

COMMUNICATION

View Article Online
View Journal



Cite this: DOI: 10.1039/c5cc08439c

Received 11th October 2015,
Accepted 8th December 2015

DOI: 10.1039/c5cc08439c

www.rsc.org/chemcomm

# Biochemistry-inspired direct synthesis of nitrogen and phosphorus dual-doped microporous carbon spheres for enhanced electrocatalysis†

Yun-Pei Zhu,[ab] Yu-Ping Liu[a] and Zhong-Yong Yuan*[ab]

**Polydopamine-derived N,P-codoped microporous carbon spheres are rationally synthesized through the self-polymerization of dopamine induced by the phosphonic species, showing efficient performance towards electrocatalytic oxygen reduction and hydrogen evolution reactions, due to the well-developed porosity and doping effect.**

Weakening the high dependence of modern society on conventional fossil fuels represents a worldwide target of high priority, which has initialized a variety of advanced technologies for sustainable energy conversion and storage, such as metal-air batteries, fuel cells, and water electrolysis.[1] The key fact of these technologies and devices lies in a series of electrochemical processes, for instance, oxygen reduction reaction (ORR) and hydrogen evolution reaction (HER). Noticeably, Pt exhibits considerable electrocatalytic activity along with low overpotential and fast reaction kinetics towards both ORR and HER, though the low abundance as well as unfavorable price prohibit the application potential. Actually tremendous endeavor has been devoted to developing cost-effective alternatives to substitute noble Pt, transition-metal-based materials have been well spotted due to the various crystalline phases and the corresponding fantastic electron properties;[2] however, the deterioration susceptibility and low electrical conductivity greatly prevent their practical utilization. A new category beyond metals has been recognized as a promising candidate for Pt so as to broaden the selection range of catalytic systems.[3]

Featuring adjustable molecular structures, metal-free carbonaceous materials have been investigated for designated catalysis ranging from organic synthesis to electrochemistry.[4] Furthermore, the introduction of porosity into carbons can efficiently improve reaction processes owing to optimized mass transport and well-exposed active sites, among which micropores associated with a large surface area are essential for high energy conversion and storage.[5] Although hard-templating and physical/chemical activation methods are capable of enhancing the microporosity,[6] the constraints of typical synthesis are complication and involvement of toxic reagents. On the other side, the intentional engineering of pristine carbons through chemical doping in the carbonaceous backbone, such as N, P, B, and S, is a promising route to tailor the electronic characteristics and thus the apparent electrochemical activities.[7] Particularly, the codoping of two different heteroatoms, *e.g.*, N and P, into the carbon backbones can induce a synergistic effect between the two elements, accordingly resulting in much enhanced electrocatalytic activity.[7] However, the establishment of effective, yet controllable methodologies for the rational synthesis of heteroatom-doped microporous carbons in a manner of low costs and natural friendliness remains challenging.

Dopamine, a kind of biomolecule that contains amine and catechol functional groups, can easily self-polymerize under alkaline conditions to generate polydopamine (PDA), which can ideally perform as a carbon precursor to prepare N-doped carbons upon carbonization.[8] Indeed, the codoping of two elements within the carbonaceous framework can remarkably boost the electrocatalytic performance, due to the synergistic effect between the heteroatoms by inducing larger asymmetrical spin and charge density relative to single doping.[9] Nonetheless, there is still scarce study focused on heteroatom-codoped carbons depending on dopamine polymerization chemistry towards electrochemistry to the best of our knowledge. Herein, taking advantage of the strong and versatile self-polymerization capability of dopamine, we demonstrate our attempts to prepare N,P-codoped microporous carbon spheres (NP-MCS) in the presence of soft templates, wherein organophosphonic species serve as both P source and pH buffer. The resultant molecular peculiarity and textual properties of NP-MCS ensure excellent activity and durability for use as electrocatalysts in ORR and HER.

[a] *Key Laboratory of Advanced Energy Materials Chemistry (Ministry of Education), Collaborative Innovation Center of Chemical Science and Engineering (Tianjin), College of Chemistry, Nankai University, Tianjin 300071, China. E-mail: zyyuan@nankai.edu.cn*

[b] *National Institute for Advanced Materials, School of Materials Science and Engineering, Nankai University, Tianjin 300353, China*

† Electronic supplementary information (ESI) available: Detailed experimental procedures and additional figures. See DOI: 10.1039/c5cc08439c

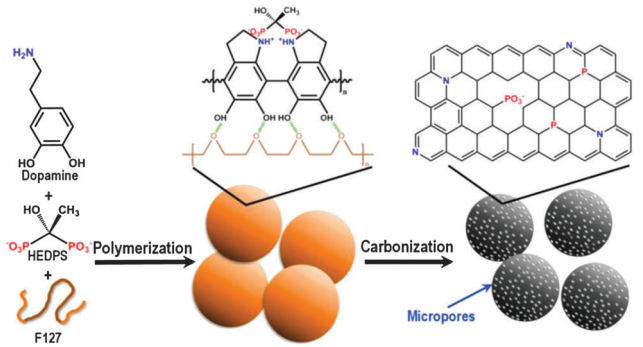


Fig. 1 Schematic synthesis process of N,P-codoped microporous carbon spheres.

Note that the organophosphonic moieties, as herein presented as sodium salt hydroxyethylidene diphosphonic acid (HEDPS), can be reversely protonized or alkalized (Fig. S1, ESI†), signifying the capability for pH buffering. Correspondingly, the addition of dopamine monomers into the basic HEDPS solution can mildly initialize the polymerization reaction; the amine functional groups in dopamine facilitate the easy incorporation of organophosphonic linkages because of the acid–base interaction with phosphoric sites (Fig. 1). As illustrated in the Fourier transform infrared (FT-IR) spectrum (Fig. S2, ESI†), the characteristic spectral peaks of functional groups including N–H and C–N bonds can be identified in the pristine polydopamine, while the typical amine bonds weaken, accompanied by the appearance of weak phosphate vibrations in the HEDPS-incorporated polydopamine, suggesting the intimate linking from both components. The strong interactions between polymerized species and block copolymers can favor the introduction of templates with high molecular weight. Further calcination under the protection of nitrogen is capable of carbonization and introduction of heteroatoms into the carbon backbones.

The scanning electron microscopic (SEM) image (Fig. 2a) shows that the NP-MCS material obtained exhibits structural integrity and spherical morphology with a diameter of 300–400 nm, consistent with the observation from transmission electron microscopic (TEM) analysis (Fig. 2b). Further magnification reveals the smooth surface of the carbon sphere (Fig. 2c), while the high-resolution TEM (HR-TEM) graph in Fig. 2d shows that NP-MCS possesses micropore channels, but with no detectable mesopores or macropores. Energy-dispersive X-ray (EDX) mapping confirms that N and P elements are effectively introduced and homogeneously distributed throughout the carbon sphere matrix at the nanoscale (Fig. S3, ESI†).

X-ray photoelectron spectroscopy (XPS) measurements were performed to identify the stoichiometry and chemical state. As depicted in Fig. 3a, the C 1s fine spectra for NP-MCS can be deconvoluted into four components, *i.e.*, 284.6 eV ($sp^2$-hybridized graphitic C), 285.9 eV (N-$sp^2$ C), 286.8 eV (C═O), and 288.7 eV (O–C═O).[3] Fitting of N 1s spectra indicates the existence of pyridinic N, quaternary N, and pyridinic-*N*-oxides, attributable to binding energies of 397.8, 400.1, and 403.4 eV, respectively (Fig. 3b).[3,9] For the P 2p region spectra, the dominant contribution

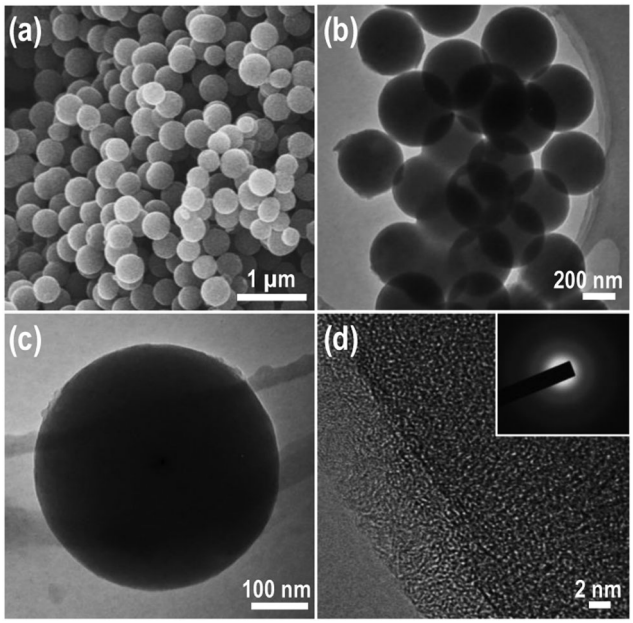


Fig. 2 SEM (a) and TEM (b–d) images of NP-MCS. Inset of (d) shows the selected area electron diffraction (SAED) pattern.

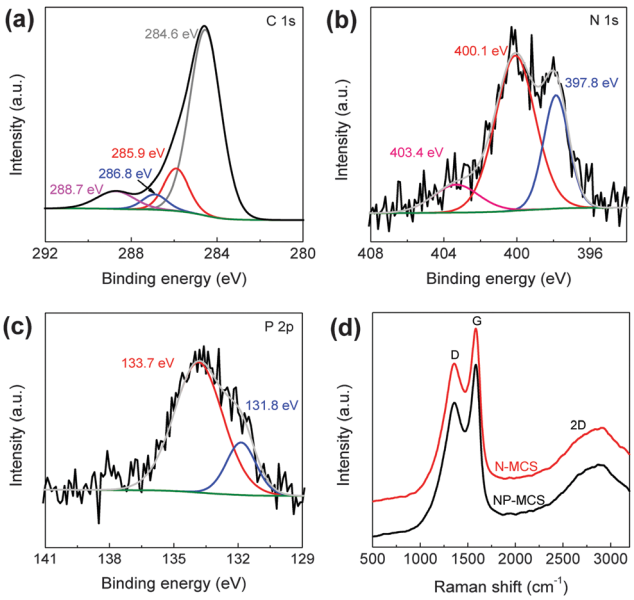


Fig. 3 (a–c) High-resolution XPS spectra of C 1s, N 1s, and P 2p in NP-MCS. (d) Raman spectra of N-MCS and NP-MCS.

locating at 133.7 eV can be assigned to phosphate-like structures bound to carbon lattices, as well as a shoulder at 131.8 eV corresponding to the P–C bond (Fig. 3c).[7] These functional groups as detected by XPS are indicative of carbons that contain N and P heteroatoms chemically bonded in the carbonaceous network.

Indeed, chemical doping can result in the variation of electronic structures, as evidenced by Raman spectroscopy. Fig. 3d demonstrates two sharp peaks in the Raman spectrum at low frequency of 1360 $cm^{-1}$ (D band) and 1585 $cm^{-1}$ (G band), ascribed to the imperfections in $sp^2$ carbon structures and the $E_{2g}$ vibrational

mode of graphitic carbon atoms, respectively, whereas the wide 2D band located at around 2700 $cm^{-1}$ at the high frequency is associated with graphitic carbons.[3] The graphitic property is further illustrated by X-ray diffraction (XRD), which shows one broad peak at $2\theta$ = 24.2° and the other weak diffraction at around $2\theta$ = 41° (Fig. S4, ESI†), characteristic of graphitic carbon materials with a low degree of graphitization. Moreover, the downshift of the G band in comparison with pristine carbons provides additional evidence for the defective structures resulting from the doping effect.[10] By calculating the ratio of intensities of the D band and the G band ($I_D/I_G$), the relative degree of disorder/order can be determined. The increased $I_D/I_G$ value of NP-MCS (1.51) relative to that of the N-doped counterpart (1.43), prepared in the absence of a phosphonic reagent (denoted as N-MCS, Fig. S5 and S6, ESI†), can be related to the additional P modification.

$N_2$ adsorption–desorption isotherms were collected to evaluate the textual properties of the synthesized carbons. The sorption isotherm for NP-MCS is of typical H1 together with significant adsorption below relative pressure ($P/P_0$) < 0.1 (Fig. S7, ESI†), due to the capillary filling of micropores. There are almost no hysteresis loops in the medium $P/P_0$ range, revealing the absence of mesoporosity in the resulting carbons. Accordingly, the pore size distribution curve shows a maximum at around 1.3 nm. The $N_2$ condensation close to atmospheric pressure in the adsorption branch means the presence of cavities between the spheres. Of note is that NP-MCS possesses a higher Brunauer–Emmett–Teller (BET) specific surface area of 634 $m^2\ g^{-1}$ than that of N-MCS (542 $m^2\ g^{-1}$), indicating that introducing P heteroatoms into the carbonaceous framework can efficiently improve the textural properties.[11] Although soft templates are employed in the typical synthesis, mesostructures cannot be reasonably achieved. It should be noted that PDA can robustly adhere on a diversity of matrix,[12] as herein on supermolecular copolymers (Fig. 1). Further polymerization reaction can significantly disturb the general self-assembly behavior of block copolymers that is driven by relatively weak intermolecular interaction, leading to the unfolding of copolymer supermolecules and thus inducing the embedding of block chains into the polydopamine. The removal of the template molecules upon calcination can result in the generation of microporosity, as the block chains of triblock copolymers are able to cause some disfigurement on the pore wall of the final products.[13] In comparison with NP-MCS, the much lower specific surface area of the carbonaceous material prepared in the absence of F127 further confirms the positive role of template molecules in improving the resultant porosity (Fig. S8, ESI†).

Introducing heteroatoms into the porous carbon frameworks is believed to play a crucial role in elevating the electrocatalytic activity. Cyclic voltammetry (CV) is first carried out in 0.1 M KOH solution saturated with $O_2$ to evaluate the electrochemical ORR performance (Fig. 4a). Well-resolved cathodic oxygen reduction peaks appear in both cases of NP-MCS and N-MCS, whereas NP-MCS exhibits larger CV area and more positive peak potential, implying that the incorporation of the P dopant is effective in enlarging the electrocatalytically active surface area by generating additional active sites and facilitating the ORR process. In the linear sweep voltammograms (LSVs) recorded on a rotating disk electrode (RDE) (Fig. 4b), the dual-doped NP-MCS sample outperforms the singly doped N-MCS catalyst in terms of reaction current density, half-wave potential, and onset potential, coinciding well with the CV results and thereby revealing the enhanced synergistic effect of N and P codoping. Notably, the onset potential and limiting current density for NP-MCS approach the commercial Pt/C reference. A series of more detailed measurements of the RDE systems at different rotational speeds from 900 to 2500 rpm were conducted to illustrate the electrochemical oxygen reduction kinetics (Fig. S9 and S10, ESI†). The current density increases with the increase of the rotating rate because of the shortened diffusion distance at high speeds, and the electron transfer number ($n$) can be determined according to the Koutecky–Levich (K–L) equation (Fig. S9 and S10, ESI†). From the linear relationship of K–L plots, the $n$ value in one ORR process is determined to be 3.82 for NP-MCS, close to that of Pt/C (3.87), indicating the pseudo-four-electron-dominated oxygen reduction pathway.

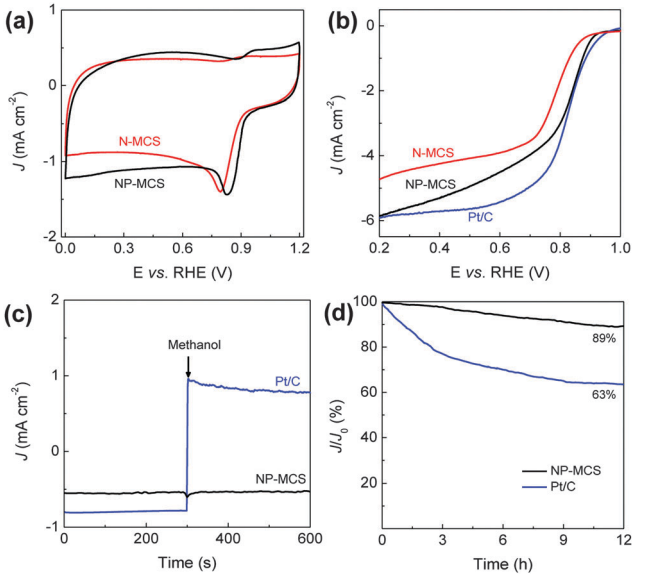


Fig. 4 (a) CV curves of NP-MCS in $O_2$-saturated 0.1 M KOH solution at a scan rate: 20 mV $s^{-1}$. (b) LSV curves of N-MCS, NP-MCS and Pt/C in $O_2$-saturated 0.1 M KOH. (Scan rate: 5 mV $s^{-1}$, rotating speed: 1600 rpm.) (c) The chronoamperometric response curves of NP-MCS and Pt/C after the instant addition of methanol. (d) The chronoamperometric responses of NP-MCS and Pt/C at 0.8 V.

High catalytic selectivity against fuel oxidation during cathodic reactions is of great importance in developing low-temperature fuel cells. For Pt/C, the cathodic current shifts to the anodic current immediately after the addition of methanol (Fig. 4c), which is accompanied by the observation of one new peak (Fig. S11, ESI†), attributed to methanol oxidation–reduction, *i.e.*, the poisoning of the noble catalyst. In sharp contrast, no activity specific to methanol happened to NP-MCS (Fig. 4c and Fig. S12, ESI†), suggesting its excellent tolerance ability to the methanol crossover effect. Moreover, the chronoamperometric response test shows that NP-MCS retains 89% of the initial

current after 12 h of continuous operation at 0.8 V, whereas Pt/C loses nearly 37% of its initial current (Fig. 4d). The strong long-term durability of the carbon-based catalyst can be ascribed to the stable chemical bonding of N and P in the carbonaceous backbone.

Additionally, the electrocatalytic activities of the carbonaceous materials towards HER were examined in acidic medium (0.5 M $H_2SO_4$). From the polarization curves and Tafel plots (Fig. S13, ESI†), NP-MCS shows certain superiority over N-MCS in both onset potential (148 *vs.* 183 mV) and Tafel slope (108 *vs.* 126 mV $dec^{-1}$). The dual-doped NP-MCS material requires an overpotential of 270 mV to realize a HER current density of 10 mA $cm^{-2}$, lower than N,P-codoped or singly doped carbons.[9a] It is noteworthy that the HER activity of NP-MCS can even rival some classical metallic catalysts, for instance, nanostructured molybdenum carbide, nickel-molybdenum nitride nanosheets, and hierarchical molybdenum disulfide microboxes.[14] In addition, both NP-MCS and N-MCS present Tafel slopes in the region of 90–130 mV $dec^{-1}$, manifesting that an initial proton adsorption (Volmer step: $H^+ + e^- \rightarrow H^*$) is the rate-controlling step of the whole HER process. The chemical doping of N and P heteroatoms endows the resultant carbons with enhanced capability to adsorb hydrogen that therefore can accelerate the most sluggish step ($H^*$ adsorption) during the whole hydrogen evolution process.[9a] Remarkably, the stable current output over 12 h of continuous operation suggests the pronounced stability of NP-MCS for HER in an acid electrolyte (Fig. S14, ESI†).

To conclude, we have disclosed an efficient strategy to prepare microporous N and P dual-doped carbon spheres, wherein the self-polymerization effect upon the stimulation of organophosphonic moieties permits the successful introduction of the dopant atom. The remarkable features of abundant porosity, chemical doping and carbonaceous framework render the microporous carbons a promising candidate for electrochemical ORR and HER with enhanced catalytic activity and long-term stability. The synthetic method described in this study towards porous carbon spheres holds the potential in exploiting alternative metal-free multifunctional electrocatalysts for renewable and sustainable energy conversion and storage applications.

This work was supported by the National Natural Science Foundation of China (21421001, 21573115), the Natural Science Foundation of Tianjin (15JCZDJC37100), the MOE Innovative Team (IRT13022), and the 111 project (B12015).

## Notes and references

1 (*a*) Y. Jiao, Y. Zheng, M. Jaroniec and S. Z. Qiao, *Chem. Soc. Rev.*, 2015, **44**, 2060; (*b*) Y. Zheng, Y. Jiao, M. Jaroniec and S. Z. Qiao, *Angew. Chem., Int. Ed.*, 2015, **54**, 52; (*c*) S. Chen, J. J. Duan, Y. H. Tang and S. Z. Qiao, *Nano Energy*, 2015, **11**, 11; (*d*) H. Liu, Y. Zheng, G. X. Wang and S. Z. Qiao, *Adv. Energy Mater.*, 2015, **5**, 1401186.

2 (*a*) M. S. Faber, R. Dziedzic, M. A. Lukowski, N. S. Kaiser, Q. Ding and S. Jin, *J. Am. Chem. Soc.*, 2014, **136**, 10053; (*b*) Y. Nie, L. Li and Z. Wei, *Chem. Soc. Rev.*, 2015, **44**, 2168; (*c*) T. Y. Ma, J. R. Ran, S. Dai, M. Jaroniec and S. Z. Qiao, *Angew. Chem., Int. Ed.*, 2014, **53**, 7281; (*d*) J. J. Duan, S. Chen, M. Jaroniec and S. Z. Qiao, *ACS Nano*, 2015, **9**, 931.

3 (*a*) Y. P. Zhu, Y. Liu, Y. P. Liu, T. Z. Ren, G. H. Du, T. Chen and Z. Y. Yuan, *J. Mater. Chem. A*, 2015, **3**, 11725; (*b*) Y. Zheng, Y. Jiao, Y. Zhu, L. H. Li, Y. Han, Y. Chen, A. Du, M. Jaroniec and S. Z. Qiao, *Nat. Commun.*, 2014, **5**, 3783.

4 L. Dai, Y. Xue, L. Qu, H. J. Choi and J. B. Baek, *Chem. Rev.*, 2015, **115**, 4823.

5 (*a*) M. Lefèvre, E. Proietti, F. Jaouen and J. P. Dodelet, *Science*, 2009, **324**, 71; (*b*) J. Shui, C. Chen, L. Grabstanowicz, D. Zhao and D. J. Liu, *Proc. Natl. Acad. Sci. U. S. A.*, 2015, **112**, 10629.

6 (*a*) L. Liu, Y. P. Zhu, M. Su and Z. Y. Yuan, *ChemCatChem*, 2015, **7**, 2765–2787; (*b*) C. Wang, L. Sun, Y. Zhou, P. Wan, X. Zhang and J. Qiu, *Carbon*, 2013, **59**, 537.

7 (*a*) T. Y. Ma, J. Ran, S. Dai, M. Jaroniec and S. Z. Qiao, *Angew. Chem., Int. Ed.*, 2015, **54**, 4646; (*b*) H. Jiang, Y. Zhu, Q. Feng, Y. Su, X. Yang and C. Li, *Chem. – Eur. J.*, 2014, **20**, 3106; (*c*) J. J. Duan, S. Chen, B. A. Chambe, G. A. Andersson and S. Z. Qiao, *Adv. Mater.*, 2015, **27**, 4234.

8 (*a*) K. Ai, Y. Liu, C. Ruan, L. Lu and G. Lu, *Adv. Mater.*, 2013, **25**, 998; (*b*) Y. Liu, K. Ai and L. Lu, *Chem. Rev.*, 2014, **114**, 5057; (*c*) J. Tang, J. Liu, C. Li, Y. Li, M. O. Tade, S. Dai and Y. Yamauchi, *Angew. Chem., Int. Ed.*, 2015, **54**, 588.

9 (*a*) Y. Zheng, Y. Jiao, L. H. Li, T. Xing, Y. Chen, M. Jaroniec and S. Z. Qiao, *ACS Nano*, 2014, **8**, 5290; (*b*) Y. Meng, D. Voiry, A. Goswami, X. Zou, X. Huang, M. Chhowalla, Z. Liu and T. Asefa, *J. Am. Chem. Soc.*, 2014, **136**, 13554.

10 M. R. Gao, Y. F. Xu, J. Jiang, Y. R. Zheng and S. H. Yu, *J. Am. Chem. Soc.*, 2012, **134**, 2930.

11 (*a*) D. Hulicova-Jurcakova, A. M. Puziy, O. I. Poddubnaya, F. Suárez-García, J. M. D. Tascón and G. Q. Lu, *J. Am. Chem. Soc.*, 2009, **131**, 5026; (*b*) Y. P. Zhu, Y. Liu, Y. P. Liu, T. Z. Ren, T. Chen and Z. Y. Yuan, *ChemCatChem*, 2015, **7**, 2903.

12 (*a*) Y. Tian, Y. Cao, Y. Wang, W. Yang and J. Feng, *Adv. Mater.*, 2013, **25**, 2980; (*b*) W. Qiang, W. Li, X. Li, X. Chen and D. Xu, *Chem. Sci.*, 2014, **5**, 3018.

13 (*a*) Y. Meng, D. Gu, F. Zhang, Y. Shi, L. Cheng, D. Feng, Z. Wu, Z. Chen, Y. Wan, A. Stein and D. Zhao, *Chem. Mater.*, 2006, **18**, 4447; (*b*) L. Liu, Q. F. Deng, T. Y. Ma, X. Z. Lin, X. X. Hou, Y. P. Liu and Z. Y. Yuan, *J. Mater. Chem.*, 2011, **21**, 16001.

14 (*a*) W. F. Chen, C. H. Wang, K. Sasaki, N. Marinkovic, W. Xu, J. T. Muckerman, Y. Zhu and R. R. Adzic, *Energy Environ. Sci.*, 2013, **6**, 943; (*b*) W. F. Chen, K. Sasaki, C. Ma, A. I. Frenkel, N. Marinkovic, J. T. Muckerman, Y. Zhu and R. R. Adzic, *Angew. Chem., Int. Ed.*, 2012, **51**, 6131; (*c*) L. Zhang, H. B. Wu, Y. Yan, X. Wang and X. W. Lou, *Energy Environ. Sci.*, 2014, **7**, 3302.

 